Journal of Hazardous Materials 278 (2014) 391–400

Contents lists available at ScienceDirect

Journal of Hazardous Materials

journal homepage: www.elsevier.com/locate/jhazmat

The influence of manganese–cobalt oxide/graphene on reducing fire hazards of poly(butylene terephthalate)

Dong Wang[a], Qiangjun Zhang[a], Keqing Zhou[a], Wei Yang[a], Yuan Hu[a,b,*], Xinglong Gong[a,c,**]

[a] State Key Laboratory of Fire Science, University of Science and Technology of China, 96 Jinzhai Road, Hefei, Anhui 230026, PR China
[b] USTC-CityU Joint Advanced Research Centre, Suzhou Key Laboratory of Urban Public Safety, Suzhou Institute for Advanced Study, University of Science and Technology of China, 166 Ren'ai Road, Suzhou, Jiangsu 215123, PR China
[c] CAS Key Laboratory of Mechanical Behaviour and Design of Materials, Department of Modern Mechanics, University of Science and Technology of China, Hefei, Anhui 230026, PR China

HIGHLIGHTS

- $MnCo_2O_4$–GNS hybrids are synthesized by a two-stage liquid phase method.
- $MnCo_2O_4$–GNS/PBT composites were prepared via a masterbatch-melt blending method.
- Fire hazards are monitored and evaluated by cone calorimeter and TG-IR.
- $MnCo_2O_4$–GNS hybrids decrease thermal hazards and smoke hazards of PBT composites.
- $MnCo_2O_4$–GNS hybrids perform better catalytic oxidation of CO and organic volatile.

ARTICLE INFO

Article history:
Received 14 March 2014
Received in revised form 22 May 2014
Accepted 26 May 2014
Available online 2 June 2014

Keywords:
$MnCo_2O_4$–GNS hybrids
Nanocomposites
Thermal hazards
Smoke hazards
Poly(butylene terephthalate)

ABSTRACT

By means of direct nucleation and growth on the surface of graphene and element doping of cobalt oxide (Co_3O_4) nano-particles, manganese–cobalt oxide/graphene hybrids ($MnCo_2O_4$–GNS) were synthesized to reduce fire hazards of poly(butylene terephthalate) (PBT). The structure, elemental composition and morphology of the obtained hybrids were surveyed by X-ray diffraction, X-ray photoelectron spectrometer and transmission electron microscopy, respectively. Thermogravimetric analysis was applied to simulate and study the influence of $MnCo_2O_4$–GNS hybrids on thermal degradation of PBT during combustion. The fire hazards of PBT and its composites were assessed by the cone calorimeter. The cone test results had showed that peak HRR and SPR values of $MnCo_2O_4$–GNS/PBT composites were lower than that of pure PBT and Co_3O_4–GNS/PBT composites. Furthermore, the incorporation of $MnCo_2O_4$–GNS hybrids gave rise to apparent decrease of pyrolysis products containing aromatic compounds, carbonyl compounds, carbon monoxide and carbon dioxide, attributed to combined impact of physical barrier for graphene and cat O_4 for organic volatiles and carbon monoxide.

1. Introduction

As is well known, Fire hazards of polymer materials are thermal hazards and smoke hazards. Thermal hazards are that polymer materials during combustion generate a large amount of heat that drives people trapped in the fire into a tremendous threat and encourages the spread of fire. Heat release rate (HRR), total heat release (THR), time to ignition, fire performance index and fire growth index are all evaluation index of thermal hazards [1,2]. Among these, HRR is the most important parameter to estimate seriousness of thermal hazards, especially peak heat release rate (PHRR) [3]. Smoke hazards are polymer materials during combustion generate a large amount of pyrolysis products composed of smoke particles, organic volatiles, carbon dioxide (CO_2), carbon monoxide (CO) and so on [4]. The hazards of organic volatiles exhibit on three aspects: firstly, organic volatiles could be condensed and aggregated to form smoke particles, which would

* Corresponding author at: State Key Laboratory of Fire Science, University of Science and Technology of China, 96 Jinzhai Road, Hefei, Anhui 230026, PR China. Tel.: +86 551 63601664; fax: +86 551 63601664.
** Corresponding author at: State Key Laboratory of Fire Science, University of Science and Technology of China, 96 Jinzhai Road, Hefei, Anhui 230026, PR China. Tel.: +86 551 63600419; fax: +86 551 63600419.
E-mail addresses: yuanhu@ustc.edu.cn (Y. Hu), gongxl@ustc.edu.cn (X. Gong).

http://dx.doi.org/10.1016/j.jhazmat.2014.05.072
0304-3894/

greatly increase the difficulty of fire rescue by reducing the visibility of fire scenes; secondly, various kinds of organic volatiles including aromatic hydrocarbons [5] and carbonyl compounds [6] are harmful for humans body; finally, organic volatiles can act as "fuel" to support burning. Hence, the reduction of organic volatiles would increase the visibility of fire scenario, lower the damage to people's health and decrease HRR of materials. Moreover, CO, the most dangerous killer for casualties in fire accidents, is the deadliest threat to persons fell into fire [7]. Therefore, decrease of organic volatiles and CO yield to reduce smoke hazards of materials, has been more and more active [4,8]. Based on the previous work, it can be seen that it is an effective and green way to catalyze organic volatiles and CO to non-flammable and non-toxic carbon dioxide (CO_2) [9–11].

Due to good dimensional stability, high thermal resistance, prominent mechanical properties and excellent electrical insulation, Poly(butylene terephthalate) (PBT) has been broadly applied in electronic industries [12]. Similar to other polymer materials, PBT has high fire hazards in the applications when fire accidents happen. PHRR of pure PBT would reach up to 1404 kW/m^2 [13], indicating that large amount of heat will be released during combustion. Yang *et al.* have demonstrated that plentiful aromatic compounds and carbonyl compounds are liberated during burning [14], which harm human's health. In addition, aromatic compounds tend to form smoke particles because of high content of carbon, thus reducing the visibility of fire scenes. Therefore, it is important to reduce fire hazards of PBT, which is in favor of enlarging its application.

As the most studied class of layered materials, graphene nanosheets (GNSs) have attracted attention in numerous fields covering catalysts, energy devices, transistor, nanocomposites [15–17]. Due to the superior barrier effect resulting from its peculiar two-dimensional (2D) structure, GNSs have aroused continuous studies on fire safety in last several years [18–20]. Kim et al. have proved that graphene nanosheets show remarkable flame resistance [21]. Besides, our previous reports have demonstrated that GNS can significantly inhibit the release of heat and pyrolysis outcomes during burning of polymer materials [22]. Whereas, flame retardant efficiency of graphene alone could not reach anticipant result. To enhance the inflaming retarding efficiency of graphene, it is essential to modify graphene with other flame retardants. Because of high efficiency in catalytic carbonization and catalytic oxidation, transition metal oxide is a nice choice [23].

As a result of high catalytic activity of tricobalt tetraoxide (Co_3O_4), it has been applied in facilitating hydrogen (H_2) production [24], promoting oxygen reduction reaction (ORR) [25], accelerating deep oxidation of CO [26] and organic volatiles [27], and so on. Among these, catalytic oxidation of CO and organic volatiles is most appealing for decreasing toxic gases. In order to improve catalytic activity of Co_3O_4, doping other transition metal element in Co_3O_4 is a more effective method. Zhao et al. show MnO_3 has better catalytic oxidation of phenol than Co_3O_4 [28]. Furthermore, substituted Co_3O_4 with Mn has shown more excellent catalytic activity for ORR [29]. As a consequence, it is reasonable to expect that doping Mn into tricobalt tetraoxide may perform better catalytic oxidation of CO and organic volatiles during the combustion of polymers. Furthermore, manganese sub-group compounds could tremendously improve flame retardance of intumescent polymer systems via increasing char residues and forming more compact char layer [30–32], which demonstrates the importance of Mn on reducing fire hazards of polymer.

In this work, the covalently coupled $MnCo_2O_4$–GNS hybrids were synthesized by the nucleation and crystallization of $MnCo_2O_4$ nanoparticles on graphene and were added into PBT to prepare $MnCo_2O_4$–GNS/PBT composites via a masterbatch-melt blending method. It is anticipated that $MnCo_2O_4$–GNS hybrids could show better catalytic oxidative activity of generated CO and organic volatiles than Co_3O_4/GNS hybrids, thus leading to lower fire hazards of PBT.

2. Experimental

2.1. Materials

Poly(butylene terephthalate) was purchased from BASF Chemical Company, Germany. Powdered graphite, oil of vitriol (98%), $NaNo_3$, $KMnO_4$, H_2O_2 solution (30%), hydrochloric acid, $Co(OAc)_2{\cdot}4H_2O$, $Mn(OAc)_2{\cdot}4H_2O$ and NH_4OH were all bought from Sinopharm Chemical Reagent Co., Ltd.

2.2. Synthesis of $MnCo_2O_4$–GNS hybrid

Graphite oxide (GO) was originated from graphite by means of modified Hummers' method. $MnCo_2O_4$–GNS hybrids were synthesized via two-stage liquid phase method, as shown in Scheme 1a. Firstly, 8 ml of 0.3 M cobalt acetate aqueous solution and 4 ml of 0.3 M manganese acetate aqueous solution were mixed with 200 ml GO ethanol suspension (∼ 0.5 mg/ml), accompanied by adding 200 ml of water and 8 ml $NH_3{\cdot}H_2O$. The reaction was held at 80 °C for the whole day with mild stirring. Secondly, the above mixture was shifted to an autoclave and kept at 150 °C for 4 h. Since then, the resultant products were collected by centrifugal separation, then cleaned with deionized water, and completely dried.

Co_3O_4–GNS hybrids were synthesized through the same procedure expect 4 ml of 0.3 M manganese acetate aqueous solution was replaced by 2 ml of 0.6 M cobalt acetate aqueous solution.

2.3. Preparation of $MnCo_2O_4$–GNS/PBT nanocomposites

Scheme 1b displays that $MnCo_2O_4$–GNS/PBT nanocomposites were processed by a masterbatch-melt blending method. 0.5 g $MnCo_2O_4$–GNS hybrids were dispersed in a certain amount of the mixed solvent composed by phenol and tetrachloroethane (the mass ratio was 1:1) with several hours of ultrasonication and mechanical agitation, and homogeneous suspension was obtained. 4.5 g PBT was dissolved in proper amount of the above-mentioned solvents and the mixture was added to the above suspension. After 2 h of ultrasonication and mechanical stirring, this homogenous mixture was obtained and dried in a vacuum oven overnight to remove excess solvents. Then the masterbatch (10% $MnCo_2O_4$–GNS hybrids and 90% PBT) was obtained and mixed with neat PBT by the melting method to prepare the samples containing 1% $MnCo_2O_4$–GNS hybrids.

Co_3O_4–GNS/PBT composites were prepared via the same step expect only $MnCo_2O_4$–GNS hybrids were replaced by the same amount of Co_3O_4–GNS.

2.4. Characterization

X-ray diffraction (XRD) measurements were implemented on a Japan Rigaku D Max-Ra rotating anode X-ray diffractometer. The scanning speed and range were 4°/min and 10°–70° respectively.

X-ray photoelectron spectrometer (XPS) spectra were recorded using a Kratos Axis Ultra DLD spectrometer employing a monochromatic Al Kα X-ray source ($h\nu$ = 1486.6 eV).

The morphology of manganese–cobalt oxide/graphene hybrid was observed by transmission electron microscopy (TEM, JEM-2100F, Japan Electron Optics Laboratory Co., Ltd., Japan).

Thermogravimetric analysis (TGA) was implement with the aid of a Q5000 IR (TA Instruments) thermal analyzer in range between indoor temperature and 800 °C. The heating speed is 20 °C/min.

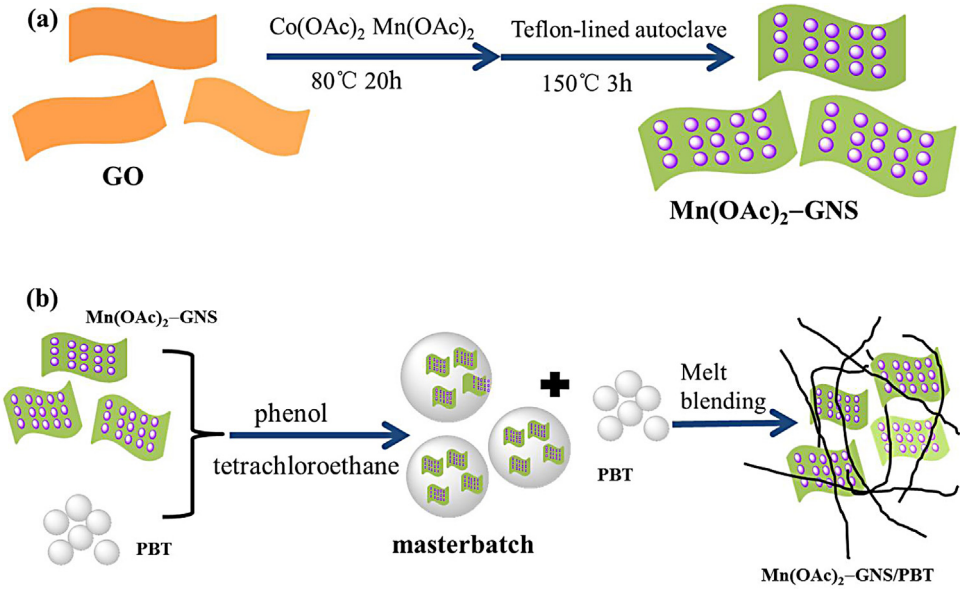

Scheme 1. Preparation process of (a) $MnCo_2O_4$–GNS hybrid and (b) $MnCo_2O_4$–GNS/PBT nanocomposites.

Fire hazards of samples were performed on a cone calorimeter (Fire Testing Technology, UK) on the basis of ASTM E1354/ISO 5660.

Thermogravimetric analysis/infrared spectrometry (TG-IR) of the samples was performed using a TGA Q5000 IR thermogravimetric analyzer that was interfaced to the Nicolet 6700 FTIR spectrophotometer through a Thermo-Nicolet TGA spectrophotometer.

3. Results and discussion

3.1. Characterization of the $MnCo_2O_4$–GNS hybrids

$MnCo_2O_4$/GNS hybrids were characterized by XRD to verify the phase, as shown in Fig. 1. The chief peaks of $MnCo_2O_4$–GNS and Co_3O_4–GNS are commendably line with the cubic spinel $MnCo_2O_4$ and Co_3O_4, respectively. The (002) diffraction peak of GNS disappears, demonstrating that evident stack is destroyed because of the formation of $MnCo_2O_4$ or Co_3O_4 nanoparticles on the face of graphene. The peaks of the former are mildly changed to lower 2θ angles than that of the latter, as a result of bigger size Mn ions. In addition, no other addition diffraction peaks have emerged in the XRD patterns of $MnCo_2O_4$–GNS and Co_3O_4–GNS hybrids, which affirms they have not been contaminated.

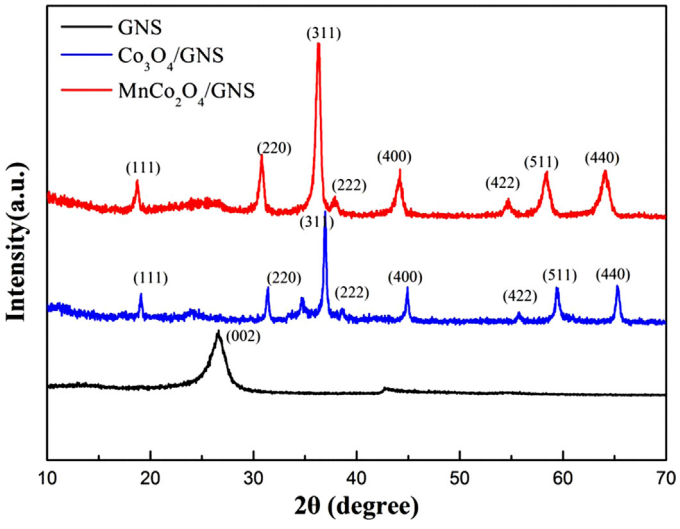

Fig. 1. XRD patterns of the as-synthesized GNS, Co_3O_4–GNS and $MnCo_2O_4$–GNS hybrids.

XPS analysis was employed to analyze elementary composition, oxidation states of metal atoms and nitrogen boding configurations of the as-synthesized $MnCo_2O_4$–GNS hybrids. Fig. 2a shows the characteristic peaks of C 1s, O 1s, N 1s, Co 2p and Mn 2p, indicating that carbon, oxygen, nitrogen, cobalt and manganese elements exist in the hybrids and the Co/Mn ratio is about 2 which is closely fitted to the designed ratio. The XPS spectrum for Co 2p shown in Fig. 2b exhibits two sharp peaks at 779.2 and 795.0 eV, belonging to Co $2p_{3/2}$ and Co $2p_{1/2}$, and two shoulder peaks with binding energies at 786.3 and 803.1 eV. In the Mn 2p spectrum (Fig. 2c), the major peak Mn $2p_{3/2}$ is at 642.2 eV and the minor one Mn $2p_{1/2}$ is at 653.5 eV. As revealed in Fig. 2d, the high resolution N 1s peak can be deconvoluted into pyridinec N, pyrrolic/amino N and graphitic N [33].

Fig. 3 shows microstructure of graphene and $MnCo_2O_4$–GNS hybrids. As could be observed in Fig. 3a, GNS shows typically flat yet folded nanosheets with a few hundred nanometers size. As regards $MnCo_2O_4$–GNS hybrids (Fig. 3b), it can be seen that many dark nanoparticles of uniform size are decorated on the face of GNS and overlaps of graphene nanosheets are validly inhibited.

3.2. Thermal decomposition of $MnCo_2O_4$–GNS/PBT nanocomposites

TGA was used to simulate and study thermal decomposition of PBT and its nanocomposites during burning. TG/DTG profiles of PBT and its composites are displayed in Fig. 4. As can be observed, all the samples have two stages on the basis of DTG profiles, which is corresponding to the pyrolysis of the polymer macromolecules and the oxidation of char residue, respectively. Almost 95 wt% of the total mass loss happens in the temperature scope between 350 °C and 450 °C. After incorporating Co_3O_4–GNS or $MnCo_2O_4$–GNS hybrids into PBT, the onset degradation temperature (T_{onset}) where the mass loss is 5% are lower than pure PBT, corresponding to a 5 and 9 °C decrement, which is caused by the excellent heat conductivity of graphene to speed up diffusion of heat through PBT matrix [34]. Moreover, the DTG profiles (Fig. 4b) demonstrate the

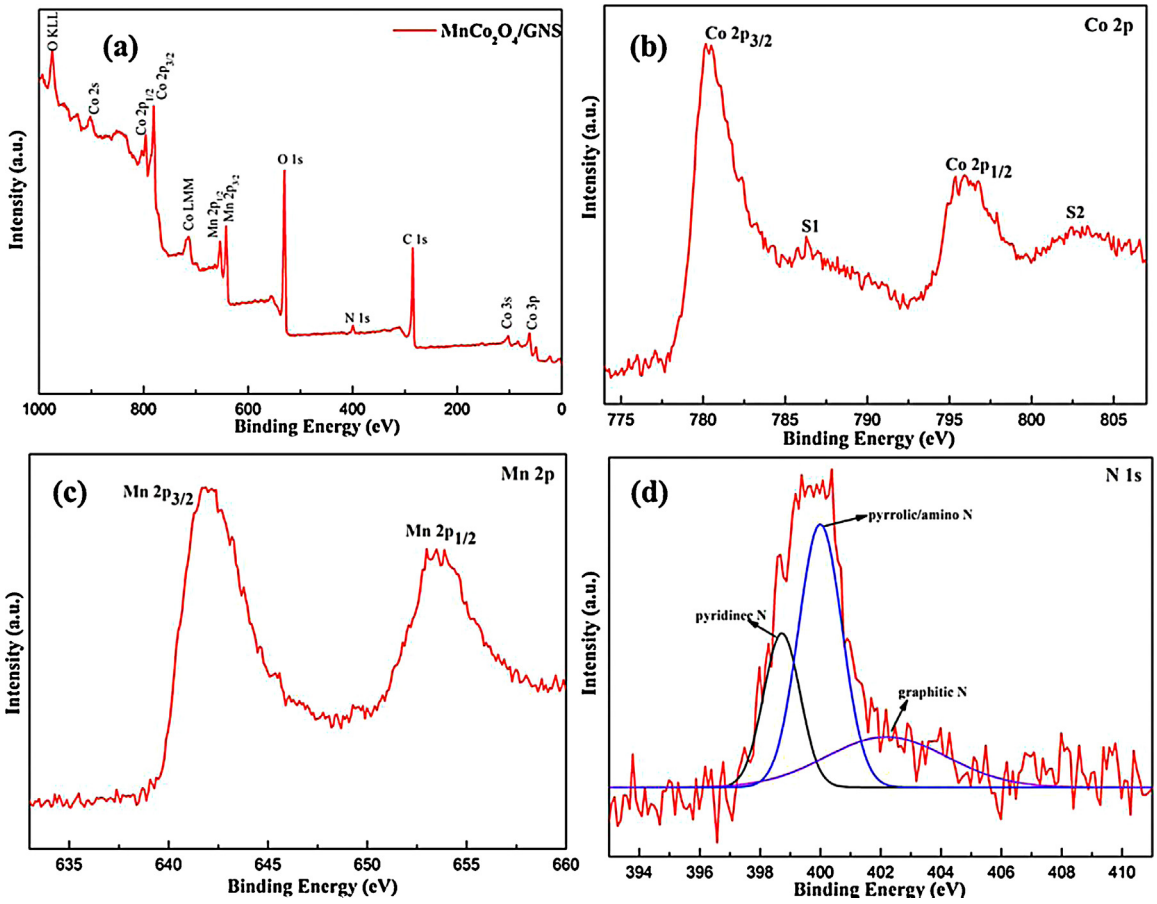

Fig. 2. XPS spectra of the as-synthesized $MnCo_2O_4$–GNS hybrid (a), high resolution Co 2p (b), Mn 2p (c) and N1s (d) of XPS spectra of the as-synthesized $MnCo_2O_4$–GNS hybrids, respectively.

maximum weight loss rates of Co_3O_4–GNS/PBT and $MnCo_2O_4$–GNS/PBT are lower than that of pure PBT, depending on the synergistic effect of physical barrier of GNS and catalytic carbonization of transition metal oxides to prevent weight loss during thermal decomposition [35,36]. Meanwhile, an interesting finding is that the largest weight loss rate of $MnCo_2O_4$–GNS/PBT is inferior to that of Co_3O_4–GNS/PBT, possibly ascribed to formation of the more compact barrier by doped Mn.

As is well known, the oxidization of graphene at elevated temperature is the most serious challenge to the barrier effect of GNS. In order to confirm that physical barrier effect of GNS works during the thermal pyrolysis course of PBT, thermal oxidation of graphene was investigated by TGA, as displayed in Fig. 5. Pure GNS exhibits a successional weight loss which results from the evaporation of water and subsequent oxidation of the resultant char. At the temperature of the maximum decomposition rate of PBT and its composites

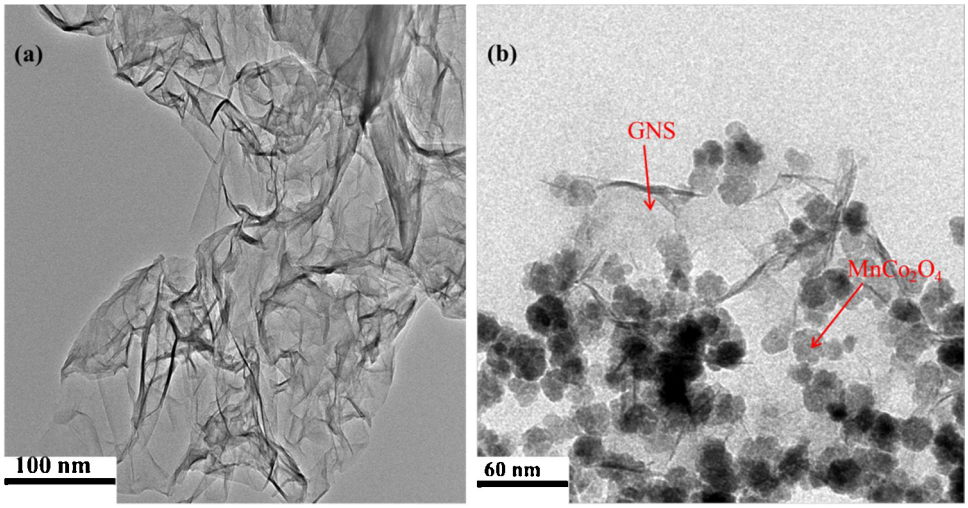

Fig. 3. TEM image of GNS (a) and $MnCo_2O_4$–GNS hybrids (b).

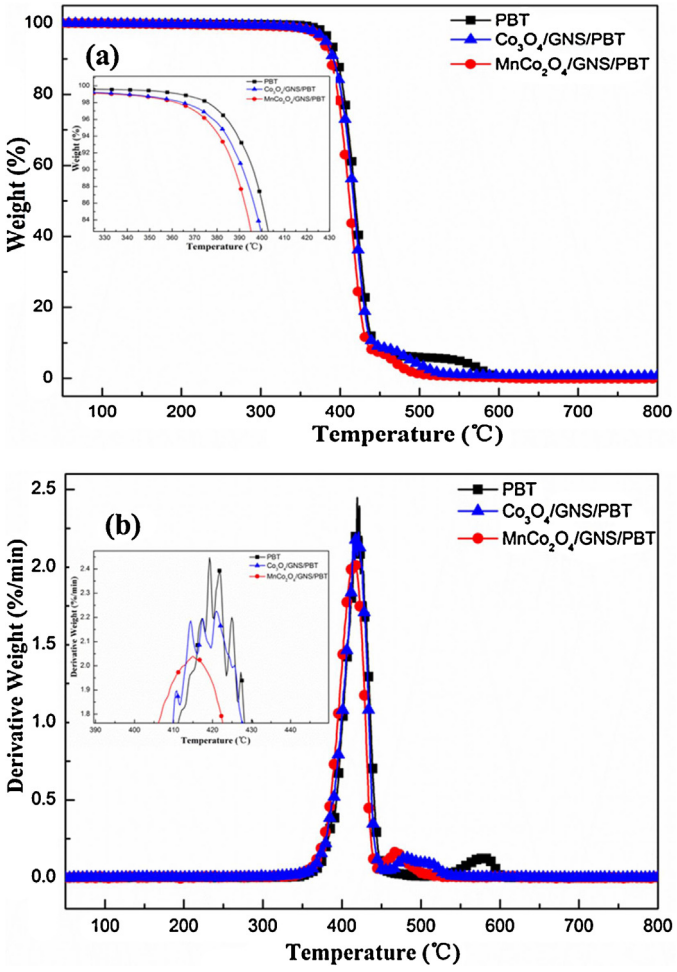

Fig. 4. TG (a) and DTG (b) profiles of PBT and its composites as a function of temperature under air atmosphere.

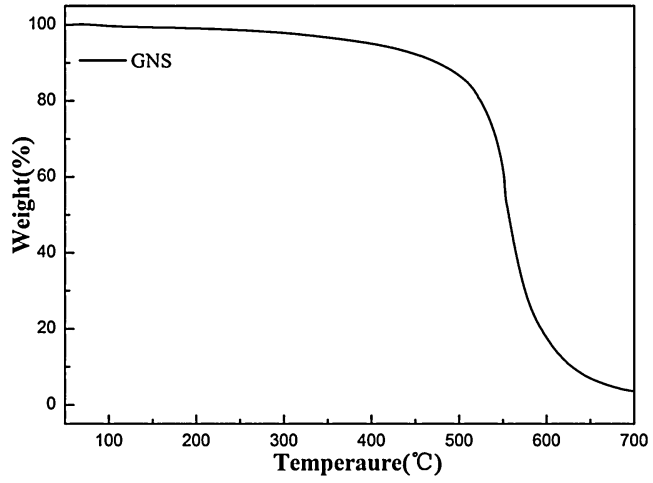

Fig. 5. TG versus time curves of GNS under air atmosphere.

(T_{max}, around 420 °C), the residual content of GNS still reaches up to 88.8%, proving that thermal oxidation of graphene has few impact on the physical barrier of graphene at the maximum decomposition stage.

3.3. Fire hazards of PBT and its composites

The cone calorimeter is a commonly employed equipment for assessing fire hazards of materials in real-world fire situations. HRR, THR and Smoke production rate (SPR) are employed to monitor the fire hazards of materials in real time. PHRR and peak smoke production rate (PSPR) are two foremost parameters for evaluating thermal hazards and smoke hazards of materials, respectively [37]. As is well known, the lower values of PHRR, the smaller heat release, the less thermal hazards of materials; the lower values of PSPR, the better visibility of fire scenes, the less smoke hazards of materials. HRR, SPR, THR versus time and FPI versus FGI curves of PBT and its nanocomposites are presented in Fig. 6, and these vital data gotten from cone tests are also recorded in Table 1. As can be observed in Fig. 6a, pure PBT burns very rapidly and the PHRR value reaches up to 1539 kW/m^2, manifesting that PBT is one of inflammable materials with high thermal hazards. After incorporating 1% Co_3O_4–GNS hybrids into PBT, the PHRR value is decreased to 1071 kW/m^2, with a 30.4% reduction compared to pure PBT. Moreover, the PHRR value of $MnCo_2O_4$–GNS/PBT composites is further reduced to 966 kW/m^2, corresponding to a 39.4% reduction. Similar to the change trend of PHRR, the PSPR value of Co_3O_4–GNS/PBT composites is decreased by 19.4% and that of $MnCo_2O_4$–GNS/PBT composites is lowest with a 35.7% reduction. The decreasing PHRR and PSPR are greatly related to compact degree of char and more compact of char indicates less PHRR and PSPR. Herein, compact degree of char are investigated by SEM (Fig. 7). The char layer of pure PBT is loose with many porous holes that provide channels for the release of smoke particles, flammable pyrolysis products and generated heat. Nevertheless, the introduction of Co_3O_4–GNS gives rise to a continuous and tight char layer except some holes. Besides, char layers of $MnCo_2O_4$–GNS are more compact with no pores, which demonstrates doped Mn facilitates formation of compact char layers. The compact char layers could inhibit escape of smoke particles, flammable gas and heat.

To some degree, TTI (time to ignition) and total heat release are also generally utilized to assess fire hazards of materials. The longer of TTI and the lower of THR mean the less of fire hazards. The TTI of Co_3O_4–GNS/PBT and $MnCo_2O_4$–GNS/PBT composites are a little shorter than neat PBT, because the high thermal conductivity of GNS could speed-up the volatilization of inflammable gas. Compared to neat PBT, the incorporation of 1% Co_3O_4–GNS results in the lower THR, and the addition of 1% $MnCo_2O_4$–GNS/PBT leads to further lower THR. The above phenomenon could be interpreted by catalytic carbonization of Co_3O_4–GNS and $MnCo_2O_4$–GNS hybrids to result in less "fuel" to support burning. The explanation is verified by the different char yields of samples, as displayed in digital photos (Fig. 7) of char residues. Pure PBT burns completely with little char residues, while the char residues of Co_3O_4–GNS/PBT composites are more than that of pristine PBT, and the $MnCo_2O_4$–GNS/PBT composites have the maximum char residues among all the samples. The increased char residues could be interpreted by catalytic carbonization of Co_3O_4–GNS and $MnCo_2O_4$–GNS hybrids. Obviously,

Table 1
Cone data for PBT, Co_3O_4–GNS/PBT and $MnCo_2O_4$–GNS/PBT composites.

Sample	TTI (s)	PHRR (kW/m^2)	PSPR (m^2/s)	THR (MJ/m^2)	FGI (kW/m^2/s)	FPI (kW/m^2/s)
PBT	68	1539	0.577	68.4	10.3	22.6
Co_3O_4/GNS/PBT	66	1071	0.465	64.7	7.8	16.2
$MnCo_2O_4$/GNS/PBT	65	966	0.371	62.7	7.3	14.9

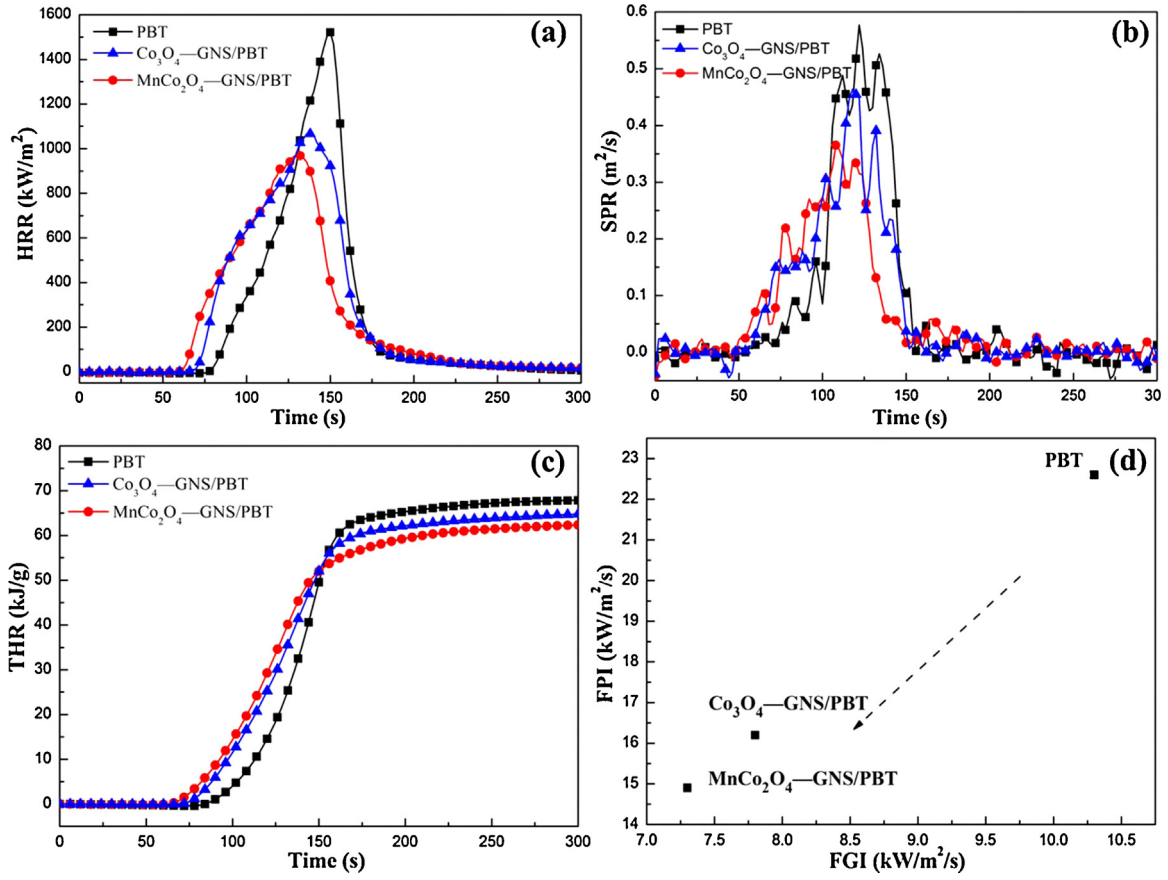

Fig. 6. HRR (a), SPR (b) and THR (c) curves of PBT and its nanocomposites, and fire performance based on FPI versus FGI curves of PBT and its composites.

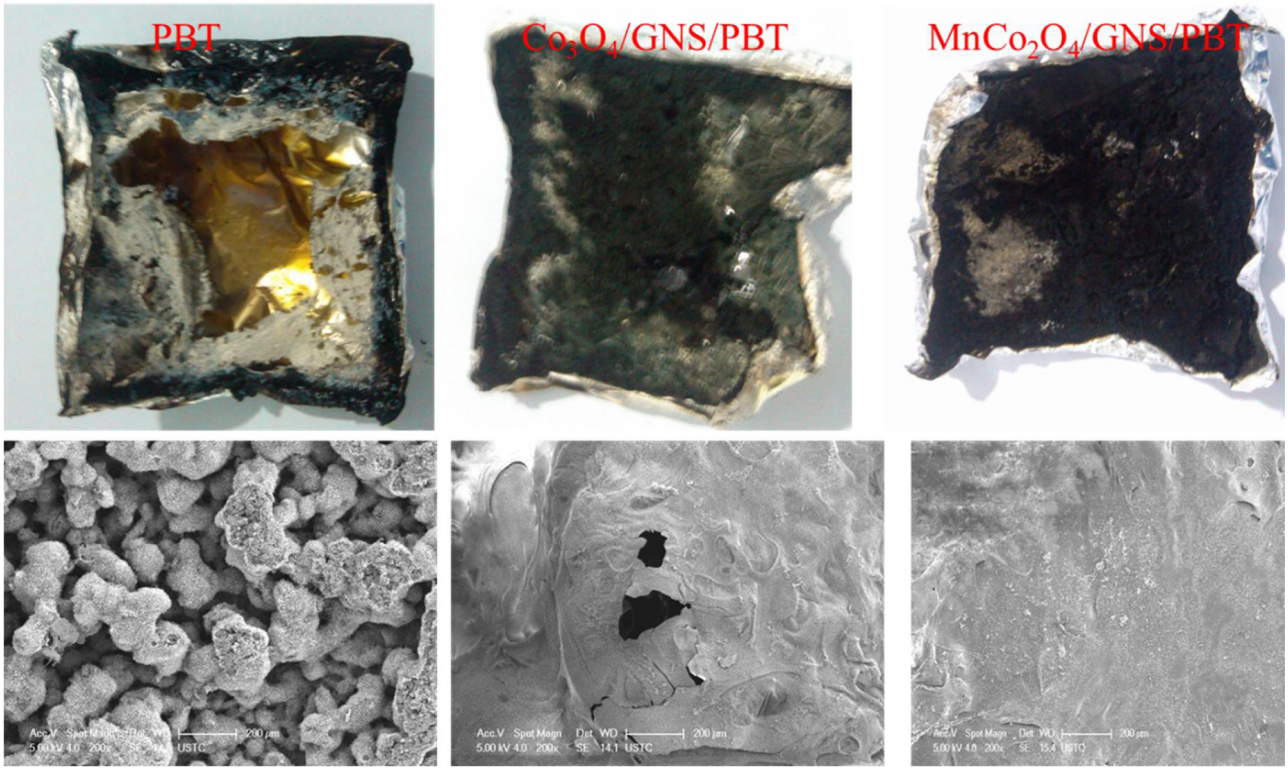

Fig. 7. Digital photos of PBT, Co_3O_4–GNS/PBT and $MnCo_2O_4$–GNS/PBT composites after the cone tests.

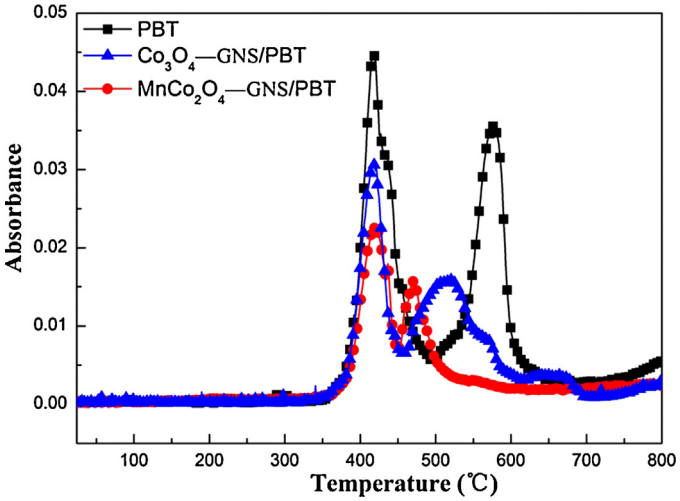

Fig. 8. Absorbance of decomposition products versus temperature for PBT and its composites (Gram–Schmidt).

doped Mn would promote more char residues production of flaming PBT.

FPI and FGI, which are the ratio of PHRR to TTI and the ratio of PHRR to TTP (time to PHRR) respectively, are both important indexes for characterizing the thermal hazards of materials. It is broadly acknowledged that the larger FPI and FGI for polymer materials, the higher their thermal hazards. Following the orientation pointed by the arrow in the Fig. 6d, it is realized that the thermal hazards of $MnCo_2O_4$–GNS/PBT composites are the lowest.

3.4. Smoke hazards estimated by TG-IR

Because the cone calorimeter could measure smoke hazards of materials on the visibility of fire scenes but not on the toxicity of pyrolysis gas, TG-IR was widely used to analyze them during the thermal decomposition process of polymer materials. As can be observed in Fig. 8, pure PBT and its composites show two significant peaks of gas emission, caused by the pyrolysis of the polymer macromolecules and the oxidation of char residues respectively, which matches well with TGA results. Just as expected, the addition of Co_3O_4–GNS hybrids into PBT leads to the significant decrease of the intensity of gas emission due to the corporate properties of physical barrier of graphene nanosheets and catalytic property of cobaltous oxide. Furthermore, the intensity of gas emission of $MnCo_2O_4$–GNS/PBT composites is much lower than Co_3O_4–GNS/PBT composites, probably because $MnCo_2O_4$ shows better catalytic activity than Co_3O_4, which agrees well with TGA results.

FTIR spectra gained at the first and second maximum evolution rate in pyrolysis process of PBT and its composites are displayed in Fig. 9. Gaseous pyrolysis products emitted from PBT and its composites are recognized clearly by featured FTIR signals, such as —C—H groups for alcohols, acids and various hydrocarbons (3100–2800 cm^{-1}), carbon dioxide (2360 and 670 cm^{-1}), carbon monoxide (2180 cm^{-1}), aromatic compounds (1608, 1578, 1510, 1460, 913, 871 and 735 cm^{-1}) and carbonyl compounds (1762, 1745, 1267, 1185 and 1103 cm^{-1}) and water (4000–3500 cm^{-1}). During the thermal decomposition process, various organic volatiles including aromatic compounds and carbonyl compounds, CO_2 and CO are escaped from PBT, as exhibited in Fig. 9a. Fig. 9b reveals CO_2 is mainly emitted from matrix during the oxidation of char residues.

To further comprehend the influence of $MnCo_2O_4$–GNS and Co_3O_4–GNS hybrids on amount variation of decomposition gas, the absorbance of gaseous volatiles for PBT and its composites versus temperature is displayed in Fig. 10. The absorbance intensities of pyrolysis gas for Co_3O_4–GNS/PBT and $MnCo_2O_4$–GNS/PBT composites are much lower than that for pure PBT, which is probably due to the corporate properties of physical barrier for graphene nanosheets and catalytic properties of Co_3O_4 and $MnCo_2O_4$. The reduction of organic volatiles (aromatic compounds and carbonyl compounds) for Co_3O_4–GNS/PBT composites leads to the inhibition of smoke particles, thus benefiting the visibility of fire scenes. Importantly, the reduction of aromatic compounds and carbonyl compounds gives rise to toxic decrement of pyrolysis products, which would be helpful for fire rescue. Moreover, the reduction of aromatic compounds and carbonyl compounds results in a decrease in HRR, which decreased the fire hazards during combustion. Simultaneously, the maximum intensities of aromatic compounds and carbonyl compounds for $MnCo_2O_4$–GNS/PBT composites are lower than that for Co_3O_4–GNS/PBT composites, demonstrating that $MnCo_2O_4$–GNS hybrids shows better catalytic oxidation of organic volatiles than Co_3O_4–GNS hybrids. In terms of toxicity, carbon monoxide is much more dangerous than aromatic

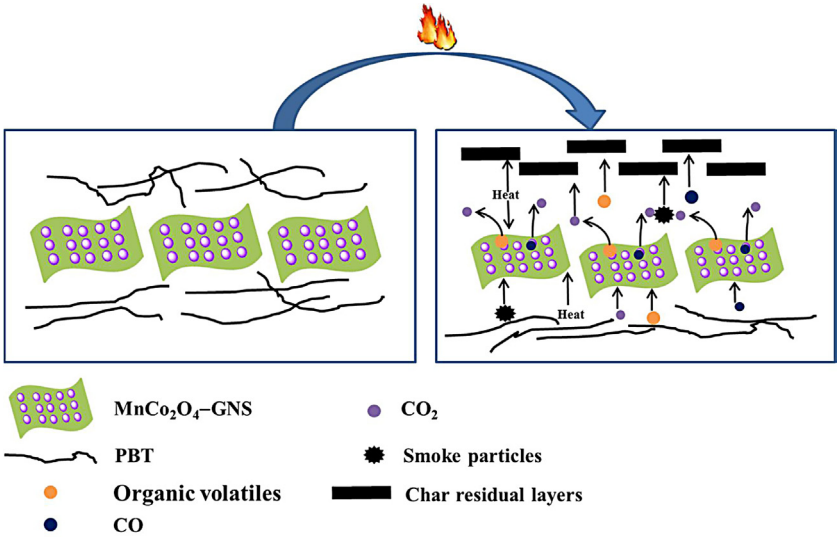

Scheme 2. Schematic illustration of the possible mechanism of the reduced fire hazards of $MnCo_2O_4$–GNS/PBT composites.

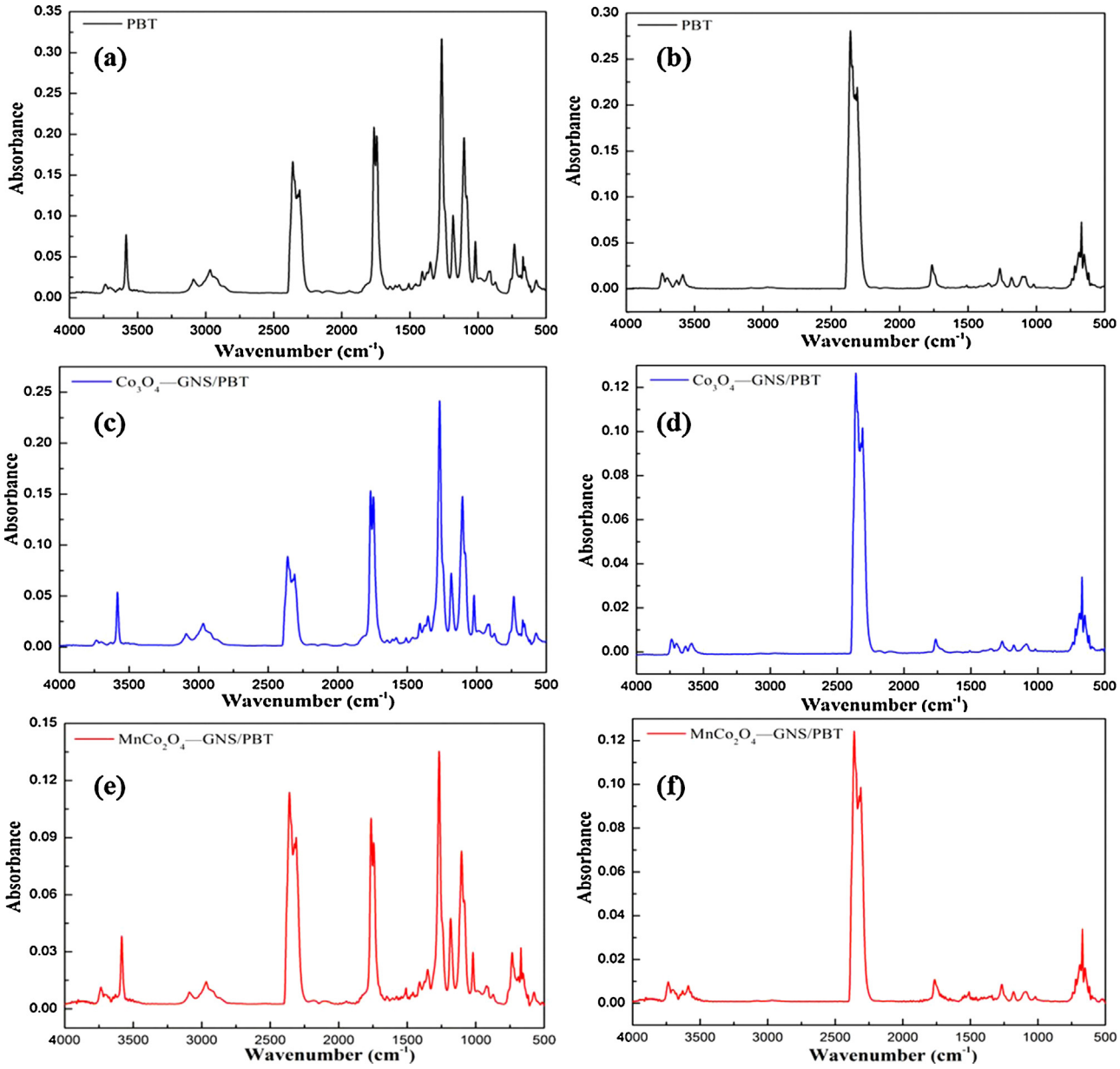

Fig. 9. FTIR spectra of decomposition products released from PBT and its composites at (a, c, e) the first maximum evolution rate and (b, d, f) the second maximum evolution rate.

compounds and carbonyl compounds. CO production for Co_3O_4–GNS/PBT composites is quite lower than that for neat PBT, attributed to two aspects: for one thing, the CO molecule is absorbed by the Co^{3+}cation in Co_3O_4 and then the adsorbent CO is oxidized by attracting the surface oxygen that might be coordinated with trivalent chromic ion [26]; for another the CO molecule is absorbed by GNS and inhibited by the barrier of GNS. As expected, CO production for $MnCo_2O_4$–GNS/PBT composites is lower than that for Co_3O_4–GNS/PBT composites, probably due to high catalytic activity of $MnCo_2O_4$ for CO oxidation. The reduction of toxic CO in pyrolysis products will be beneficial for fire rescue when fire accidents happen. Additionally, CO_2 release at the maximum decomposition of the macromolecular chains for Co_3O_4/GNS/PBT and $MnCo_2O_4$/GNS/PBT composites are much lower than that for pristine PBT, possibly ascribed to the absorption and the barrier effect of GNS. Moreover, it can be seen that CO_2 release for $MnCo_2O_4$–GNS/PBT composites is higher than that for Co_3O_4–GNS/PBT composites, also confirming that $MnCo_2O_4$ shows better catalytic activity for organic volatiles and CO oxidation to CO_2.

3.5. Flame retardant mechanism

In summary, the possible mechanism of the reduced thermal hazards and smoke hazards of $MnCo_2O_4$–GNS/PBT composites are proposed as shown in Scheme 2. During the combustion of $MnCo_2O_4$–GNS/PBT composites, organic volatiles (mainly consist of aromatic compounds and carbonyl compounds), CO, CO_2 and smoke particles released from PBT matrix are inhibited by the physical barrier effect of GNS nanosheets. Besides, organic volatiles and CO would be deeply oxidized to non-toxic CO_2 by the catalytic oxidation of $MnCo_2O_4$. Moreover, the effective barrier effect of graphene nanosheets would suppress the generated heat release and prevent the nether materials from forward burning. As well, the catalytic carbonization of $MnCo_2O_4$–GNS hybrids would facilitate the formation of compact char layers on the surface of polymers

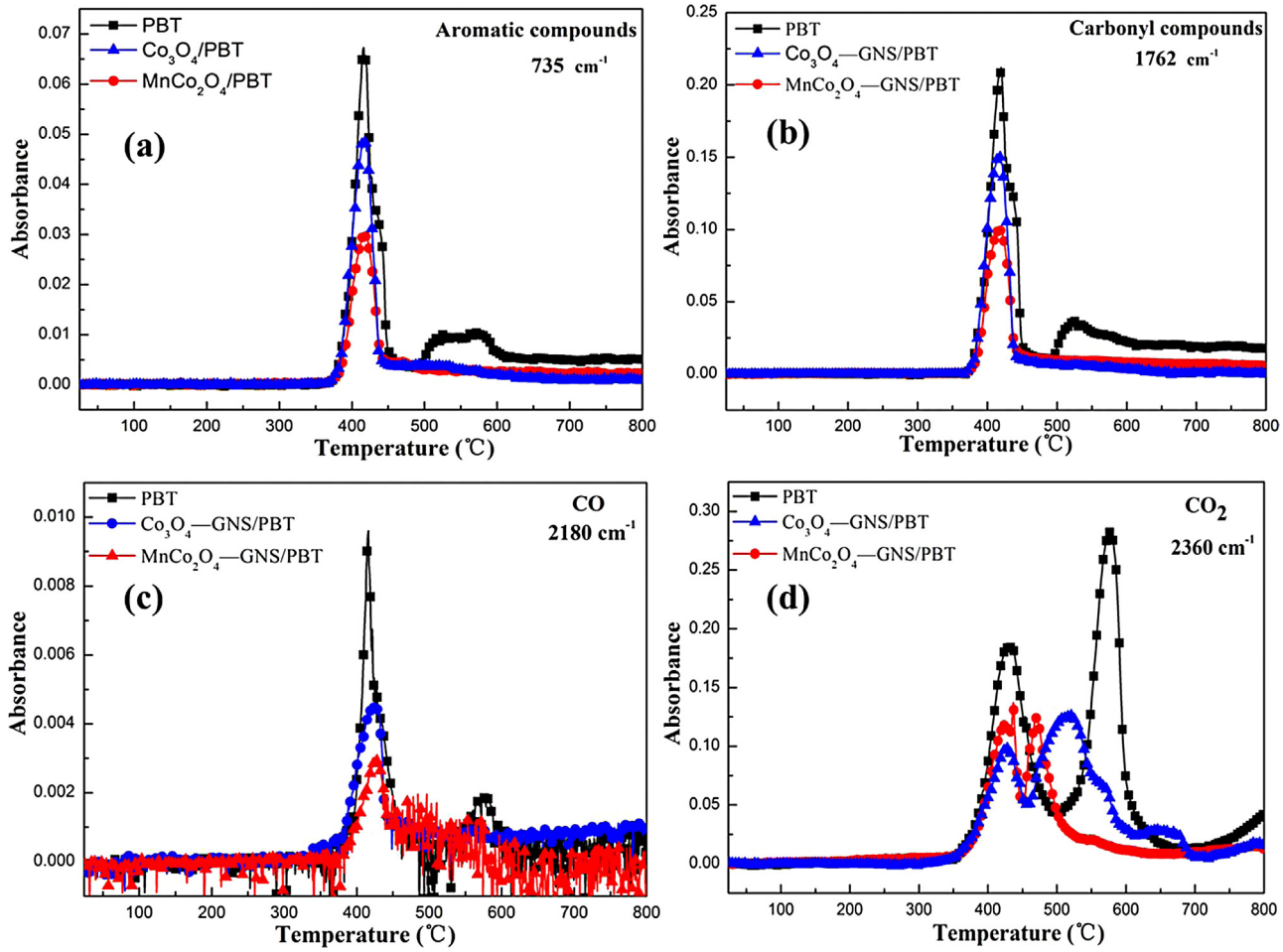

Fig. 10. Absorbance of pyrolysis products for PBT, Co_3O_4–GNS/PBT and $MnCo_2O_4$–GNS/PBT composites as a function of temperature: (a) aromatic compounds, (b) carbonyl compounds, (c) CO and (d) CO_2.

to inhibit the release of heat and pyrolysis products, and stop the underlying materials from further combustion. Meanwhile, the catalytic carbonization could decrease the combustion degree of $MnCo_2O_4$–GNS/PBT composites to cause the reduction of the total heat release which is beneficial for the enhancement of fire resistance. The comparison of fire hazards of Co_3O_4–GNS/PBT and $MnCo_2O_4$–GNS/PBT composites shows that doped Mn could enhance catalytic carbonization, improve compactness of char and strengthen catalytic activity of organic volatiles and CO.

4. Conclusion

Herein, $MnCo_2O_4$–GNS hybrids were successfully synthesized by a two-stage solution method and then added into PBT matrix via a masterbatch-melt blending method. TEM results showed that $MnCo_2O_4$ nanoparticles of uniform size were well decorated on the surface of graphene nanosheets. Thermal degradation of PBT was studied and physical barrier of GNS still works at the temperature of the maximum decomposition rate of PBT. Thermal hazards and smoke hazards of $MnCo_2O_4$–GNS/PBT composites were assessed by the cone test. When $MnCo_2O_4$–GNS hybrids were incorporated into PBT matrix, the peak HRR and SPR values of $MnCo_2O_4$–GNS/PBT composites were obviously decreased by 39.4 and 35.7%, respectively. Furthermore, smoke hazards on toxicity of pyrolysis products for PBT and its composites were analyzed by TG-IR technology. Organic volatiles and CO were deeply oxidized to non-flammable and non-toxic CO_2 by $MnCo_2O_4$–GNS hybrids, which would reduce the toxicity of pyrolysis products, thus benefiting fire rescues. Finally, the possible mechanism of the reduced thermal hazards and smoke hazards of $MnCo_2O_4$/GNS/PBT composites were attributed to physical barrier of graphene nanosheets, catalytic oxidation activity of $MnCo_2O_4$ nanoparticles and catalytic carbonization of $MnCo_2O_4$–GNS hybrids. This work would provide a simply effective solution to extend the application of graphene in reducing fire hazards of materials.

Acknowledgments

The work was financially supported by National Natural Science Foundation of China (21374111), National Basic Research Program of China (973 Program) and National Natural Science Foundation of China (51203146).

References

[1] K.C. Tsai, Orientation effect on cone calorimeter test results to assess fire hazard of materials, J. Hazard. Mater. 172 (2009) 763–772.
[2] N.N. Hong, Y. Pan, J. Zhan, B.B. Wang, K.Q. Zhou, L. Song, Y. Hu, Fabrication of graphene/Ni–Ce mixed oxide with excellent performance for reducing fire hazard of polypropylene, RSC Adv. 3 (2013) 16440–16448.
[3] J.J. Ma, J.X. Yang, Y.W. Huang, K. Cao, Aluminum-organophosphorus hybrid nanorods for simultaneously enhancing the flame retardancy and mechanical properties of epoxy resin, J. Mater. Chem. 22 (2012) 2007–2017.
[4] Y.Y. Dong, Z. Gui, Y. Hu, Y. Wu, S.H. Jiang, The influence of titanate nanotube on the improved thermal properties and the smoke suppression in poly(methyl methacrylate), J. Hazard. Mater. 209 (2012) 34–39.

[5] D.L. Zhang, T.C. An, M. Qiao, B.G. Loganathan, X.Y. Zeng, G.Y. Sheng, J.M. Fu, Source identification and health risk of polycyclic aromatic hydrocarbons associated with electronic dismantling in Guiyu town, South China, J. Hazard. Mater. 192 (2011) 1–7.
[6] M. Kitwattanavong, T. Prueksasit, D. Morknoy, T. Tunsaringkarn, W. Siriwong, Health risk assessment of petrol station workers in the inner city of bangkok, Thailand, to the exposure to BTEX and carbonyl compounds by inhalation, Hum. Ecol. Risk Assess. 19 (2013) 1424–1439.
[7] M. Braubach, A. Algoet, M. Beaton, S. Lauriou, M.E. Heroux, M. Krzyzanowski, Mortality associated with exposure to carbon monoxide in WHO European Member States, Indoor Air 23 (2013) 115–125.
[8] X. Wang, L. Song, H.Y. Yang, W.Y. Xing, H.D. Lu, Y. Hu, Cobalt oxide/graphene composite for highly efficient CO oxidation and its application in reducing the fire hazards of aliphatic polyesters, J. Mater. Chem. 22 (2012) 3426–3431.
[9] S.R. Zhang, J.J. Shan, Y. Zhu, L. Nguyen, W.X. Huang, H. Yoshida, S. Takeda, F. Tao, Restructuring transition metal oxide Nanorods for 100% selectivity in reduction of nitric oxide with carbon monoxide, Nano Lett. 13 (2013) 3310–3314.
[10] C. George, A. Genovese, A. Casu, M. Prato, M. Povia, L. Manna, T. Montanari, CO oxidation on Colloidal Au0.80Pd0.20-Fe_xO_y dumbbell nanocrystals, Nano Lett. 13 (2013) 752–757.
[11] M. Konsolakis, S.A.C. Carabineiro, P.B. Tavares, J.L. Figueiredo, Redox properties and VOC oxidation activity of Cu catalysts supported on Ce1-xSmxOdelta mixed oxides, J. Hazard. Mater. 261 (2013) 512–521.
[12] P. Liu, M.M. Liu, C. Gao, F. Wang, Y.F. Ding, B. Wen, S.M. Zhang, M.S. Yang, Preparation, characterization and properties of a halogen-free phosphorous flame-retarded poly(butylene terephthalate) composite based on a DOPO derivative, J. Appl. Polym. Sci. 130 (2013) 1301–1307.
[13] E. Gallo, U. Braun, B. Schartel, P. Russo, D. Acierno, Halogen-free flame retarded poly(butylene terephthalate) (PBT) using metal oxides/PBT nanocomposites in combination with aluminium phosphinate, Polym. Degrad. Stab. 94 (2009) 1245–1253.
[14] W. Yang, L. Song, Y. Hu, H.D. Lu, Investigations of thermal degradation behavior and fire performance of halogen-free flame retardant poly(1,4-butylene terephthalate) composites, J. Appl. Polym. Sci. 122 (2011) 1480–1488.
[15] B. Zheng, J. Wang, F.B. Wang, X.H. Xia, Synthesis of nitrogen doped graphene with high electrocatalytic activity toward oxygen reduction reaction, Electrochem. Commun. 28 (2013) 24–26.
[16] S.Y. Yang, K.H. Chang, H. Wen Tien, Y.F. Lee, S.M. Li, Y.S. Wang, C.C. Hu, Design and tailoring of a hierarchical graphene-carbon nanotube architecture for supercapacitors, J. Mater. Chem. 21 (2011) 2374–2380.
[17] K.T. Kim, J.W. Jung, W.H. Jo, Synthesis of graphene nanoribbons with various widths and its application to thin-film transistor, Carbon 63 (2013) 202–209.
[18] Y.M. Shi, L.J. Li, Chemically modified graphene: flame retardant or fuel for combustion? J. Mater. Chem. 21 (2011) 3277–3279.
[19] S. Liu, H.Q. Yan, Z.P. Fang, H. Wang, Effect of graphene nanosheets on morphology, thermal stability and flame retardancy of epoxy resin, Compos. Sci. Technol. 90 (2014) 40–47.
[20] S.Y. Ran, C. Chen, Z.H. Guo, Z.P. Fang, Char barrier effect of graphene nanoplatelets on the flame retardancy and thermal stability of high-density polyethylene flame-retarded by brominated polystyrene, J. Appl. Polym. Sci. 131 (2014), http://dx.doi.org/10.1002/app.40520.
[21] F. Kim, J.Y. Luo, R. Cruz-Silva, L.J. Cote, K. Sohn, J.X. Huang, Self-propagating domino-like reactions in oxidized graphite, Adv. Funct. Mater. 20 (2010) 2867–2873.
[22] Y.Q. Guo, C.L. Bao, L. Song, B.H. Yuan, Y. Hu, In situ polymerization of graphene, graphite oxide, and functionalized graphite oxide into epoxy resin and comparison study of on-the-flame behavior, Ind. Eng. Chem. Res. 50 (2011) 7772–7783.
[23] L. Wang, L. Song, Y. Hu, K.K. Richard, Yuen, Influence of different metal oxides on the thermal, combustion properties and smoke suppression in Ethylene-Vinyl Acetate, Ind. Eng. Chem. Res. 52 (2013) 8062–8069.
[24] M. Casas-Cabanas, G. Binotto, D. Larcher, A. Lecup, V. Giordani, J.M. Tarascon, Defect chemistry and catalytic activity of nanosized Co_3O_4, Chem. Mater. 21 (2009) 1939–1947.
[25] Y.Y. Liang, Y.G. Li, H.L. Wang, J.G. Zhou, J. Wang, Tom Regier, H.J. Dai1, Co_3O_4 nanocrystals on graphene as a synergistic catalyst for oxygen reduction reaction, Nature 10 (2011) 780–786.
[26] X.W. Xie, Y. Li, Z.Q. Liu, M. Haruta, W.J. Shen, Low-temperature oxidation of CO catalysed by Co_3O_4 nanorods, Nature 458 (2009) 746–749.
[27] T. Garcia, S. Agouram, J.F. Sanchez-Royo, R. Murillo, A.M. Mastral, A. Aranda, I. Vazquez, A. Dejoz, B. Solsona, Deep oxidation of volatile organic compounds using ordered cobalt oxides prepared by a nanocasting route, Appl. Catal. A: General 386 (2010) 16–27.
[28] E. Saputra, S. Muhammad, H.Q. Sun, H.M. Ang, S.B. Wang, A comparative study of spinel structured Mn_3O_4, Co_3O_4 and Fe_3O_4 nanoparticles in catalytic oxidation of phenolic contaminants in aqueous solutions, J. Colloid Interface Sci. 407 (2013) 467–473.
[29] H.L. Wang, Y. Yang, Y.Y. Liang, G.Y. Zheng, Y.G. Li, Y. Cui, H.J. Dai, Rechargeable Li–O_2 batteries with a covalently coupled $MnCo_2O_4$–graphene hybrid as an oxygen cathode catalyst, Energy Environ. Sci. 5 (2012) 7931–7935.
[30] P. Zhang, L. Song, H.D. Lu, Y. Hu, Synergistic effect of nanoflaky manganese phosphate on thermal degradation and flame retardant properties of intumescent flame retardant polypropylene system, Polym. Degrad. Stab. 11 (2008) 201–207.
[31] C.X. Lu, J. Wang, L. Chen, Q. Fu, X.F. Cai, The effect of adjuvant on the halogen-free intumescent flame retardant ABS/PA6/SMA/APP blend, J. Appl. Polym. Sci. 118 (2010) 1552–1560.
[32] C.M. Feng, Y. Zhang, D. Liang, S.W. Liu, J.R. Xu, Flame retardancy and thermal degradation behaviors of polypropylene composites with novel intumescent flame retardant and manganese dioxide 104 (2013) 59–67.
[33] Y.Y. Liang, H.L. Wang, J.G. Zhou, J. Wang, Tom Regier, H.J. Dai1, Covalent hybrid of spinel manganese-cobalt oxide and graphene as advanced oxygen reduction electrocatalysts, J. Am. Chem. Soc. 134 (2012) 3517–3523.
[34] C.L. Bao, L. Song, C.A. Wilkie, B.H. Yuan, Y.Q. Guo, Y. Hu, X.L. Gong, Graphite oxide, graphene, and metal-loaded graphene for fire safety applications of polystyrene, J. Mater. Chem. 22 (2012) 16399.
[35] C.L. Bao, Y.Q. Guo, B.H. Yuan, Y. Hu, L. Song, Functionalized graphene oxide for fire safety applications of polymers: a combination of condensed phase flame retardant strategies, J. Mater. Chem. 22 (2012) 23057.
[36] J. Gong, K. Yao, J. Liu, Z.W. Jiang, X.C. Chen, X. Wen, E. Mijowska, N.N. Tian, T. Tang, Striking influence of Fe_2O_3 on the catalytic carbonization of chlorinated poly(vinyl chloride) into carbon microspheres with high performance in the photo-degradation of Congo red, J. Mater. Chem. A. 1 (2013) 5247–5255.
[37] D. Wang, K.Q. Zhou, W. Yang, W.Y. Xing, Y. Hu, X.L. Gong, Surface modification of graphene with layered molybdenum disulfide and their synergistic reinforcement on reducing fire hazards of epoxy resins, Ind. Eng. Chem. Res. 52 (2013) 17882–17890.